Flight Control Design for Small-Scale Helicopter Using Disturbance Observer Based Backstepping

Hao Lu[1]
Beihang University, Beijing, 100191, China

Cunjia Liu[2]
Loughborough University, Loughborough, LE11 3TU, United Kingdom

Lei Guo[3]
Beihang University, Beijing, 100191, China

Wen-Hua Chen[4]
Loughborough University, Loughborough, LE11 3TU, United Kingdom

[1] Ph.D. Candidate, School of Instrumentation Science and Opto-Electronics Engineering, luhao@aspe.buaa.edu.cn.
[2] Lecturer, Department of Aeronautical and Automotive Engineering; visiting researcher, School of Automation Science and Electrical Engineering, Beihang University, Beijing, 100191, China, c.liu5@lboro.ac.uk (Corresponding Author).
[3] Professor, National Key Laboratory on Aircraft Control Technology, lguo@buaa.edu.cn.
[4] Professor, Department of Aeronautical and Automotive Engineering; visiting professor, School of Automation Science and Electrical Engineering, Beihang University, Beijing, 100191, China, w.chen@lboro.ac.uk.

Nomenclature

$a,\ b$	= longitudinal and lateral flapping angles of main rotor, deg
$A_b,\ B_a$	= cross-coupled rotor flapping derivatives, $1/s$
$A_{lat},\ A_{lon}$	= cross-coupled and control derivatives for longitudinal flapping angle, deg/s
$B_{lat},\ B_{lon}$	= control and cross-coupled derivatives for lateral flapping angle, deg/s
$d_p,\ d_q,\ d_r$	= normalized lumped moment disturbances along x_b, y_b, and z_b body axes, deg/s^2
$d_x,\ d_y,\ d_z$	= normalized lumped force disturbances along x_b, y_b, and z_b body axes, m/s^2
d_F	= vector of lumped force disturbances; $[\ d_x\ \ d_y\ \ d_z\ ]^T$, m/s^2
d_M	= vector of lumped moment disturbances; $[\ d_p\ \ d_q\ \ d_r\ ]^T$, deg/s^2
$F,\ F_0$	= normalized external force and aerodynamic force, m/s^2
g	= acceleration of gravity, m/s^2
I	= inertia matrix; $diag\{I_{xx},\ I_{yy},\ I_{zz}\}$, $kg \cdot m^2$
$I_{xx},\ I_{yy},\ I_{zz}$	= roll, pitch and yaw moments of inertia, $kg \cdot m^2$
$L_a,\ M_b$	= cross-coupled derivatives for roll and pitch moments, $1/s^2$
$L_b,\ M_a$	= control derivatives for roll and pitch moments, $1/s^2$
m	= helicopter mass, kg
$M,\ M_0$	= normalized external moment and aerodynamic moment, deg/s^2
$N_{col},\ N_{ped}$	= collective control and pedal control derivatives for yaw moment, deg/s^2
N_r	= damping derivative for yaw moment, $1/s$
$p,\ q,\ r$	= angular rates of roll, pitch, and yaw, deg/s
P	= vector of helicopter position components; $[\ x\ \ y\ \ z\ ]^T$, m
T	= normalized main rotor thrust, m/s^2
$u_{col},\ u_{ped}$	= collective pitch and pedal control inputs; range $[-1,\ 1]$
$u_{lat},\ u_{lon}$	= lateral and longitudinal cyclic control inputs; range $[-1,\ 1]$
$v_x,\ v_y,\ v_z$	= helicopter velocity components along x_e, y_e, and z_e earth axes, m/s
V	= vector of helicopter velocity components; $[\ v_x\ \ v_y\ \ v_z\ ]^T$, m/s
$x,\ y,\ z$	= helicopter position components along x_e, y_e, and z_e earth axes, m
β	= vector of flapping angles; $[\ a\ \ b\ ]^T$, deg
τ	= main rotor time constant, s

ϕ, θ, ψ = Euler angles of roll, pitch, and yaw, deg

Φ = vector of Euler angles; $[\ \phi\ \ \theta\ \ \psi\ ]^T$, deg

Ω = vector of angular rates; $[\ p\ \ q\ \ r\ ]^T$, deg/s

$\|\cdot\|$ = Euclidean norm

Subscript

c = command signal

d = desired signal

ref = reference signal

Superscript

$\hat{}$ = estimate value

$\tilde{}$ = estimation error

I. Introduction

Recent years have witnessed increasing research activities in the area of small-scale helicopters since they are popular autonomous platforms for various flying missions. Compared to their full size counterparts, small-scale helicopters are more susceptible to aerodynamic uncertainties, external disturbances, and other adverse factors due to their low inertia and limited power, which in turn necessitates the development of more stable and robust flight control systems. To this end, this note adopts the disturbance observer based control scheme to enhance the flight control performance. This method is known as an active "anti-disturbance" strategy where the lumped disturbances from various sources are estimated by a disturbance observer (DO) and then incorporated into a nominal controller to compensate for their adverse effects [1–3]. A preliminary study has demonstrated the disturbance rejection ability of this control strategy on a small-scale helicopter [4].

The classical disturbance observer, such as that shown in [4], is constructed given that all the system states are measurable, but this assumption may not be true for systems like helicopters. To damp the fast dynamics and improve the stability of a scaled-down helicopter, the main rotor is commonly augmented by the Bell-Hiller mechanism which provides a derivative feedback for roll and pitch responses. In general, the main rotor dynamics can be characterised by two flapping

angles. For a small-scale helicopter with a rigid rotor head, such rotor dynamics represent a lumped flapping effect primarily introduced by the Bell-Hiller flybar and are therefore more significant [5, 6]. Unfortunately, the flapping angles are not directly measured by onboard sensors, which leaves an open problem in control design. Some early studies tend to ignore the flapping dynamics and assume these angles can be directly controlled [7, 8], but a common practice is to use the quasi-steady approximation by setting the derivatives of flapping angles to zero [4, 9, 10]. Nevertheless, completely neglecting the transient response may degrade the control performance especially when flapping dynamics are relatively slow with the increased flybar diameter and weight. To this end, the output feedback control method is adopted based on the linear model [11, 12]. Another attempt reported in [13] develops an extended Kalman filter to estimate the flapping angles. However, the unmeasurable state still remains an open problem for the disturbance observer design.

To exploit the flapping dynamics in helicopter control design, this note proposes a novel disturbance observer design that extends the scope of the classical one to partial-state unmeasurable system. The unknown external disturbances and system states can be estimated simultaneously and asymptotically. Although this information can be incorporated into many conventional controllers to enhance robustness [3], the recursive backstepping method is employed as a baseline controller due to the cascaded structure of helicopter dynamics. In this work, command filtered backstepping (CFBS) [14] is adopted. Compared to the standard backstepping, the CFBS introduces command filters that not only eliminate the tedious analytic derivative computation of virtual control signals, but also impose physical constraints on them if necessary. The design procedure of the composite controller for a small-scale helicopter is detailed in this note and its performance is demonstrated in a demanding trajectory tracking scenario. It should be noted that although demonstrated on a small-scale helicopter in this note, the disturbance observer technique can be readily applied to other aircraft to improve control robustness.

II. Helicopter Model

The flight control design is based on a general mathematical model of small-scale helicopters. Its six degrees-of-freedom rigid-body model can be represented as [4, 10]

$$\dot{P} = V \tag{1a}$$

$$\dot{V} = gz_e + R(\Theta)F \tag{1b}$$

$$\dot{R}(\Theta) = R(\Theta)Sk(\Omega) \tag{1c}$$

$$\dot{\Omega} = -I^{-1}\Omega \times I\Omega + M \tag{1d}$$

where $P = [x,\, y,\, z]^T$ and $V = [v_x,\, v_y,\, v_z]^T$ are the helicopter's position and velocity in the earth reference frame, $\Theta = [\phi,\, \theta,\, \psi]^T$ represent the Euler angles, $\Omega = [p,\, q,\, r]^T$ denote the angular rates, and $z_e = [0,\, 0,\, 1]^T$. $R(\Theta) \in \mathbb{R}^{3\times 3}$ is the standard rotation matrix from the earth reference frame to the body reference frame, R_{ij} denotes the element in ith row and jth column of $R(\Theta)$, and $Sk(\Omega)$ is a skew-symmetric matrix (see [4, 10]).

The external force F and moment M in (1) are normalized by helicopter mass m and inertia matrix I, respectively. They are composed of two parts: one is the force F_0 and moment M_0 dominantly generated by the main rotor and the tail rotor, and another is the lumped disturbances originated from other force and moment contributions, such as wind turbulences and parameter uncertainties, denoted as force disturbance d_F and moment disturbance d_M, respectively. The complete expressions are [4, 5]:

$$F = \underbrace{[\ 0 \quad 0 \quad T\ ]^T}_{F_0} + \underbrace{[\ d_x \quad d_y \quad d_z\ ]^T}_{d_F} \tag{2a}$$

$$M = \underbrace{\begin{bmatrix} L_a a + L_b b \\ M_a a + M_b b \\ N_r r + N_{col} u_{col} + N_{ped} u_{ped} \end{bmatrix}}_{M_0} + \underbrace{\begin{bmatrix} d_p \\ d_q \\ d_r \end{bmatrix}}_{d_M} \tag{2b}$$

where T is the main rotor thrust controlled by collective pitch u_{col}, and u_{ped} is the pedal input. The main rotor flapping angles a and b denote the tilt of the rotor disc along longitudinal and lateral axes, respectively. For small-scale helicopters, a flybar with small airfoils attached is mounted at 90-degree to the main rotor blades, which is used to damp the cyclic inputs (u_{lon} and u_{lat}) and

enhance the stability against gust. Following the modelling methods introduced in [4, 5], the flybar dynamics can be lumped into the main rotor flapping dynamics which can be expressed as

$$\underbrace{\begin{bmatrix} \dot{a} \\ \dot{b} \end{bmatrix}}_{\dot{\beta}} = \underbrace{\begin{bmatrix} -\frac{1}{\tau} & A_b \\ B_a & -\frac{1}{\tau} \end{bmatrix}}_{A_1} \underbrace{\begin{bmatrix} a \\ b \end{bmatrix}}_{\beta} + \underbrace{\begin{bmatrix} 0 & -1 \\ -1 & 0 \end{bmatrix}}_{A_2} \underbrace{\begin{bmatrix} p \\ q \end{bmatrix}}_{\omega_2} + \underbrace{\begin{bmatrix} A_{lat} & A_{lon} \\ B_{lat} & B_{lon} \end{bmatrix}}_{B} \underbrace{\begin{bmatrix} u_{lat} \\ u_{lon} \end{bmatrix}}_{u_{cyc}} \tag{3}$$

or compactly, $\dot{\beta} = A_1\beta + A_2\omega_2 + Bu_{cyc}$ where τ is the effective rotor time constant which includes the flybar effects.

The full helicopter dynamics are characterised by the rigid body model (1), the forces and moments (2), and the flapping dynamics (3). Since the flapping dynamics, reflected in the horizontal motion, are the main focus of this note, only the control design for the longitudinal-lateral dynamics will be discussed. Therefore, extracting the relevant longitudinal-lateral dynamics yields the cascaded system:

$$\begin{cases} \dot{P}_2 = V_2 & \text{(4a)} \\ \dot{V}_2 = R_2 T + R_N d_{\bar{F}} & \text{(4b)} \\ \dot{R}_2 = R_M \omega_2 & \text{(4c)} \\ \dot{\omega}_2 = \Phi\beta + d_{\bar{M}} & \text{(4d)} \\ \dot{\beta} = A_1\beta + A_2\omega_2 + Bu_{cyc} & \text{(4e)} \end{cases}$$

where $P_2 = [x,\, y]^T$, $V_2 = [v_x,\, v_y]^T$, $R_2 = [R_{13},\ \ R_{23}]^T$, $d_{\bar{F}} = [d_x,\, d_y]^T$, $d_{\bar{M}} = [d_p,\, d_q]^T$,

$$R_N = \begin{bmatrix} R_{11} & R_{12} \\ R_{21} & R_{22} \end{bmatrix},\ R_M = \begin{bmatrix} -R_{12} & R_{11} \\ -R_{22} & R_{21} \end{bmatrix},\ \text{and } \Phi = \begin{bmatrix} L_a & L_b \\ M_a & M_b \end{bmatrix}.$$

For a particular helicopter, the derivatives $A_{(\cdot)}$, $B_{(\cdot)}$, $L_{(\cdot)}$, $M_{(\cdot)}$, $N_{(\cdot)}$, and effective rotor time constant τ can be acquired from system identification.

III. Disturbance Observer Design

Since there is no onboard sensor to measure the flapping angle β directly, it is usually approximated by using the quasi-steady form

$$\beta = -A_1^{-1}A_2\omega_2 - A_1^{-1}Bu_{cyc} \tag{5}$$

which can be found in many prior helicopter control designs [4, 9, 10]. It can be seen that the transient response has been ignored in this approximation. Therefore, if an accurate estimate of the flapping angle can be provided to the feedback design, the control performance would be improved [13]. On the other hand, small-scale helicopters are susceptible to parameter uncertainties and external disturbances, which may also degrade the flight control performance. Hence, estimating the flapping angle and lumped disturbances simultaneously and incorporating the estimates into the feedback controller provide a promising way to enhance the flight control performance. However, the classical nonlinear disturbance observer, e.g. [1], is incapable for partial-state unmeasurable systems with external disturbances, such as subsystem (4), which in turn motivates a new disturbance observer design.

The basic principle of disturbance observer design [1–3] is that an internal state with carefully designed dynamics is introduced for the lumped disturbance estimation. Inspired by this, an additional internal state for the unmeasurable state is introduced so that the novel disturbance observer for flapping angle β and roll and pitch moment disturbance $d_{\bar{M}}$ is proposed as

$$\begin{cases} \begin{bmatrix} \dot{z}_1 \\ \dot{z}_2 \end{bmatrix} = \begin{bmatrix} A_1 & 0 \\ 0 & 0 \end{bmatrix} \begin{bmatrix} \hat{\beta} \\ \hat{d}_{\bar{M}} \end{bmatrix} + \begin{bmatrix} A_2\omega_2 + Bu_{cyc} \\ 0 \end{bmatrix} - \begin{bmatrix} l_1(\omega_2) \\ l_2(\omega_2) \end{bmatrix} (\Phi\hat{\beta} + \hat{d}_{\bar{M}}) \\ \begin{bmatrix} \hat{\beta} \\ \hat{d}_{\bar{M}} \end{bmatrix} = \begin{bmatrix} z_1 \\ z_2 \end{bmatrix} + \begin{bmatrix} p_1(\omega_2) \\ p_2(\omega_2) \end{bmatrix} \end{cases} \tag{6}$$

where $\hat{\beta}$ and $\hat{d}_{\bar{M}}$ are the estimates of β and $d_{\bar{M}}$, z_1 and z_2 are the internal states of the observer, and $l_1(\omega_2)$ and $l_2(\omega_2)$ are the observer gains derived from functions $p_1(\omega_2)$ and $p_2(\omega_2)$, such that

$$l_i(\omega_2) = \frac{\partial p_i(\omega_2)}{\partial \omega_2}, i = 1, 2 \tag{7}$$

Different from all prior work in the disturbance observer design, the observer (6) estimates not only the unknown lumped moment disturbance $d_{\bar{M}}$ but also the unmeasurable state flapping angle β.

To establish the stability property of the proposed disturbance observer, estimation errors need to be examined. Define $\tilde{\beta} = \beta - \hat{\beta}$ and $\tilde{d}_{\bar{M}} = d_{\bar{M}} - \hat{d}_{\bar{M}}$ as the corresponding estimation errors. Under the assumption that the disturbance $d_{\bar{M}}$ varies slowly with respect to the observer dynamics (i.e., $\dot{d}_{\bar{M}} \simeq 0$) [1], differentiating $\tilde{\beta}$ and $\tilde{d}_{\bar{M}}$ and incorporating the system dynamics (4) yields the

estimation error dynamics:

$$\begin{bmatrix} \dot{\tilde{\beta}} \\ \dot{\tilde{d}}_{\bar{M}} \end{bmatrix} = \begin{bmatrix} A_1 - l_1(\omega_2)\Phi & -l_1(\omega_2) \\ -l_2(\omega_2)\Phi & -l_2(\omega_2) \end{bmatrix} \begin{bmatrix} \tilde{\beta} \\ \tilde{d}_{\bar{M}} \end{bmatrix} \tag{8}$$

After the estimates $\hat{\beta}$ and $\hat{d}_{\bar{M}}$ have been obtained, the force disturbance $d_{\bar{F}}$ in Eq. (4b) also needs to be estimated noting that it can be incorporated into the system whose entire states are measurable. The disturbance observer for $d_{\bar{F}}$ is designed as

$$\begin{cases} \dot{z}_3 = -l_3(V_2)(R_2 T + R_N \hat{d}_{\bar{F}}) \\ \hat{d}_{\bar{F}} = z_3 + p_3(V_2) \end{cases} \tag{9}$$

where z_3 is the internal state, $\hat{d}_{\bar{F}}$ is the estimate for $d_{\bar{F}}$, and the observer gain is determined by $l_3(V_2) = \frac{\partial p_3(V_2)}{\partial V_2}$. This form is identical to the classical one proposed in [1]. Under the assumption that the disturbance $d_{\bar{F}}$ is slowly time varying (i.e., $\dot{d}_{\bar{F}} \simeq 0$), the time derivative of the estimation error $\tilde{d}_{\bar{F}} = d_{\bar{F}} - \hat{d}_{\bar{F}}$ is

$$\dot{\tilde{d}}_{\bar{F}} = -l_3(V_2) R_N \tilde{d}_{\bar{F}} \tag{10}$$

Letting $\tilde{d} = [\tilde{\beta}^T, \tilde{d}_{\bar{M}}^T, \tilde{d}_{\bar{F}}^T]^T$ and combining Eqs. (8) and (10), the full estimation error dynamics are governed by

$$\dot{\tilde{d}} = \Xi \tilde{d} \tag{11}$$

where

$$\Xi = \begin{bmatrix} A - l_1(\omega_2)\Phi & -l_1(\omega_2) & 0 \\ -l_2(\omega_2)\Phi & -l_2(\omega_2) & 0 \\ 0 & 0 & -l_3(V_2) R_N \end{bmatrix} \tag{12}$$

The asymptotical stability of error system (11) can be guaranteed if the system matrix Ξ is a Hurwitz matrix continuous in all fixed ω_2 and V_2 [15, Definition 2.1 and Procedure 4.1]. That is, the observer gains $l_1(\omega_2)$, $l_2(\omega_2)$, and $l_3(V)$ are selected such that the two diagonal blocks of Ξ are Hurwitz stable for all fixed ω_2 and V_2. Usually, the observer gain is chosen to be constant but

nonlinear gain design is also possible. In this work the observer gain matrices are selected as

$$\begin{cases} l_1(\omega_2) = diag\{k_1, k_2\}\Phi^{-1} \\ l_2(\omega_2) = diag\{k_3, k_4\} \\ l_3(V_2) = diag\{k_5, k_6\}R_N^{-1} \end{cases} \tag{13}$$

where $k_i \in \mathbb{R}^+, i = 1, ..., 6$ are the observer gain parameters. By integrating the observer gains listed in (13), the corresponding observer functions are obtained as $p_1(\omega_2) = l_1(\omega_2)\omega_2$, $p_2(\omega_2) = l_2(\omega_2)\omega_2$, and $p_3(V_2) = l_3(V_2)V_2$. The established stability of the error system (11) means that the estimates $\hat{\beta}$, $\hat{d}_{\bar{M}}$, and $\hat{d}_{\bar{F}}$ can approach their actual values β, $d_{\bar{M}}$, and $d_{\bar{F}}$ asymptotically regardless of the control inputs. These estimates will be incorporated into a feedback control strategy to enhance the control performance.

IV. Estimation Enhanced Command Filtered Basckstepping Control

In this section, the command filtered backstepping approach is selected to design a control law for the tracking control of the helicopter. The longitudinal-lateral subsystem (4) is a fifth-order system so that a five-step backstepping controller is built to generate the cyclic input u_{cyc} to make the helicopter track the pre-defined reference horizontal position $P_{2,ref} = [x_{ref}, y_{ref}]^T$. Applying the CFBS algorithm introduced in [14] to this subsystem results in the control laws:

$$\begin{cases} V_{2,d} = -c_P\delta_P + \dot{P}_{2,ref} & \text{(14a)} \\ R_{2,d} = T^{-1}(-c_V\delta_V - \bar{\delta}_P + \dot{V}_{2,c} - R_N\hat{d}_{\bar{F}}) & \text{(14b)} \\ \omega_{2,d} = R_M^{-1}(-c_R\delta_R - T\bar{\delta}_V + \dot{R}_{2,c}) & \text{(14c)} \\ \beta_d = \Phi^{-1}(-c_\omega\delta_\omega - R_M\bar{\delta}_R + \dot{\omega}_{2,c} - \hat{d}_{\bar{M}}) & \text{(14d)} \\ u_{cyc} = B^{-1}(-c_\beta\delta_\beta - \Phi\bar{\delta}_\omega - A_1\hat{\beta} - A_2\omega_2 + \dot{\beta}_c) & \text{(14e)} \end{cases}$$

where $V_{2,d}$, $R_{2,d}$, $\omega_{2,d}$, and β_d are the desired virtual control signals that are used to control the horizontal position, horizontal velocity, roll and pitch angle, and roll and pitch rate, respectively. $c_{(\cdot)} \in \mathbb{R}^+$ are the control gains. The tracking errors are defined as $\delta_P = P_2 - P_{2,ref}$, $\delta_V = V_2 - V_{2,c}$, $\delta_R = R_2 - R_{2,c}$, $\delta_\omega = \omega_2 - \omega_{2,c}$, and $\delta_\beta = \hat{\beta} - \beta_c$ where $V_{2,c}$, $R_{2,c}$, $\omega_{2,c}$, and β_c are the command signals that are generated sequentially. The command signals and their derivatives are produced

by virtual control signals through command filters so that these relationships can be expressed as $[\, V_{2,c} \;\; \dot{V}_{2,c} \,] = CF_1(V_{2,d})$, $[\, R_{2,c} \;\; \dot{R}_{2,c} \,] = CF_2(R_{2,d})$, $[\, \omega_{2,c} \;\; \dot{\omega}_{2,c} \,] = CF_3(\omega_{2,d})$, and $[\, \beta_c \;\; \dot{\beta}_c \,] = CF_4(\beta_d)$. CF denotes the command filter which is a second-order low-pass filter to produce the command signal and its derivative satisfying the magnitude, rate and bandwidth constraints [14].

The use of the command filter produces the difference between the command filter output and the desired virtual control signal due to the filter dynamics and constraints. For example, supposing that $V_{2,c}$ is the command filtered version of the desired virtual control signal $V_{2,d}$, their difference $V_{2,c} - V_{2,d}$ denotes the unachieved portion. The effects of these unachieved portions can be removed from the tracking errors $\delta_{(\cdot)}$ by constructing the compensating signals $\xi_{(\cdot)}$, the dynamics of which are expressed as

$$\begin{bmatrix} \dot{\xi}_P \\ \dot{\xi}_V \\ \dot{\xi}_R \\ \dot{\xi}_\omega \end{bmatrix} = \begin{bmatrix} -c_P\xi_P + (V_{2,c} - V_{2,d}) + \xi_V \\ -c_V\xi_V + T(R_{2,c} - R_{2,d}) + T\xi_R \\ -c_R\xi_R + R_M(\omega_{2,c} - \omega_{2,d}) + R_M\xi_\omega \\ -c_\omega\xi_\omega + \Phi(\hat{\beta} - \beta_d) + \Phi\xi_\beta \end{bmatrix} \tag{15}$$

where $\xi_\beta = 0$. The compensated tracking errors are defined as $\bar{\delta}_{(\cdot)} = \delta_{(\cdot)} - \xi_{(\cdot)}$. By combining (4), (14), and (15), the time derivatives of the compensated tracking errors are calculated as

$$\underbrace{\begin{bmatrix} \dot{\bar{\delta}}_P \\ \dot{\bar{\delta}}_V \\ \dot{\bar{\delta}}_R \\ \dot{\bar{\delta}}_\omega \\ \dot{\bar{\delta}}_\beta \end{bmatrix}}_{\dot{\bar{\delta}}} = \underbrace{\begin{bmatrix} -c_P & 1 & 0 & 0 & 0 \\ -1 & -c_V & T & 0 & 0 \\ 0 & -T & -c_R & R_M & 0 \\ 0 & 0 & -R_M & -c_\omega & \Phi \\ 0 & 0 & 0 & -\Phi & -c_\beta \end{bmatrix}}_{\Pi} \underbrace{\begin{bmatrix} \bar{\delta}_P \\ \bar{\delta}_V \\ \bar{\delta}_R \\ \bar{\delta}_\omega \\ \bar{\delta}_\beta \end{bmatrix}}_{\bar{\delta}} + \underbrace{\begin{bmatrix} 0 & 0 & 0 \\ 0 & 0 & R_N \\ 0 & 0 & 0 \\ \Phi & 1 & 0 \\ A_1 & 0 & 0 \end{bmatrix}}_{\Gamma} \underbrace{\begin{bmatrix} \tilde{\beta} \\ \tilde{d}_{\bar{M}} \\ \tilde{d}_{\bar{F}} \end{bmatrix}}_{\tilde{d}} \tag{16}$$

The disturbance estimates $\hat{d}_{\bar{F}}$ yielded by (9) and $\hat{d}_{\bar{M}}$ by (6) are incorporated in (14b) and (14d) to compensate for the influences of disturbances $d_{\bar{F}}$ and $d_{\bar{M}}$. As the flapping angle β is unmeasurable, it is replaced by its estimate $\hat{\beta}$ obtained from (6) in the actual cyclic input (14e). Consequently, the estimation errors $\tilde{d}_{\bar{F}}$, $\tilde{d}_{\bar{M}}$, and $\tilde{\beta}$ are coupled with compensated tracking errors in Eq. (16).

The overall structure of the disturbance observer based command filtered backstepping controller, summarized by the set of Eqs. (6), (9), and (14), can be expressed in the block diagram

shown in Fig. 1.

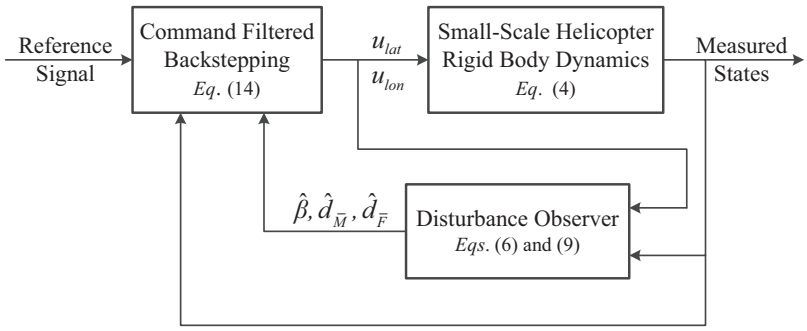

Fig. 1 Disturbance observer based command filtered backstepping control scheme

V. Stability Analysis

The stability of the resultant closed-loop system developed in Section IV is now analyzed. First, the compensated tracking errors (16) can be written into the compact form:

$$\dot{\bar{\delta}} = \Pi\bar{\delta} + \Gamma\tilde{d} \tag{17}$$

Considering $\tilde{d}$ as the input to system (17), the remaining $\dot{\bar{\delta}} = \Pi\bar{\delta}$ is the original unforced system. Using $V(\bar{\delta}) = \frac{1}{2}\bar{\delta}^T\bar{\delta}$ as a Lyapunov function candidate, the derivative of V along the trajectory of $\dot{\bar{\delta}} = \Pi\bar{\delta}$ is

$$\begin{aligned}\dot{V}(\bar{\delta}) = \frac{1}{2}\bar{\delta}^T(\Pi^T + \Pi)\bar{\delta} =& - c_P\bar{\delta}_P^2 - c_V\bar{\delta}_V^2 - c_R\bar{\delta}_R^2 - c_\omega\bar{\delta}_\omega^2 - c_\beta\bar{\delta}_\beta^2 \\ \leq& max\{-c_P, -c_V, -c_R, -c_\omega, -c_\beta\}\|\bar{\delta}\|^2\end{aligned}$$

It can be concluded from [16, Theorem 4.10] that system $\dot{\bar{\delta}} = \Pi\bar{\delta}$ has a globally exponentially stable equilibrium point at the origin $\bar{\delta} = 0$. Considering $\Pi\bar{\delta}+\Gamma\tilde{d}$ is continuously differentiable and globally Lipschitz in $(\bar{\delta}, \tilde{d})$, it follows [16, Lemma 4.6] that system (17) is input-to-state stable.

Combining the estimation error system (11) and compensated tracking error system (17), the augmented closed-loop error system is expressed as

$$\begin{cases}\dot{\bar{\delta}} = \Pi\bar{\delta} + \Gamma\tilde{d} \\ \dot{\tilde{d}} = \Xi\tilde{d}\end{cases} \tag{18}$$

Since system (17), with $\tilde{d}$ as input, is input-to-state stable and system (11) is globally asymptotically stable, then the augmented error system (18) is globally asymptotically stable by following [16,

Lemma 4.7]. It should be noticed that it is the compensated tracking error $\bar{\delta}$, not the actual tracking error δ, that converges to zero. However, Theorem 2 in [14] ensures that as the natural frequency ω_n of the command filter increases, the performance of the command filtered backstepping can be made arbitrarily close to that of the standard backstepping using analytic calculation of derivatives.

VI. Simulation Studies

This section evaluates the performance of the proposed disturbance observer based command filtered backstepping. Comparison studies are carried out against the original CFBS controller. The original CFBS controller uses the quasi-steady approximation (5) to calculate the cyclic input from the desired flapping angle, which implies that it does not contain the last step (14e) of the proposed control scheme. In the simulation, the helicopter, starting from the origin, is set to track a square trajectory anticlockwise. The initial velocity is zero and the cruising velocity is up to $5\,m/s$ with abrupt turns at each corners, which will excite large flapping motions. Throughout the maneuver the altitude and heading angle are controlled to remain constant.

The simulation is based on the numerical model of the Raptor 90 small-scale helicopter where the vehicle parameters can be found in [5] (see Table 1). The overall weight of the helicopter is $9.5\,kg$, the full length of fuselage is $1410\,mm$, and the main rotor diameter is $1605\,mm$. The designed controller and observer gains are given in Table 2. Note that I_2 denotes a second-order identity matrix in the table. Because of the cascaded structural property of helicopter system and the time-scale separation principle, it is natural to select the control gain of the former step larger than that of the next step. Moreover, the observer gains k_3 and k_4 are chosen relatively large to make the flapping angle estimation faster than the disturbance estimation. The command filter parameters used for the simulation are given in Table 3. The magnitude and rate limitations are determined by the physical constraints of the state variables, and it is also natural to select a lower natural frequency ω_n for the prior step.

To illustrate the benefits of estimating the flapping angles, the first simulation is carried out without adding external disturbances and parameter uncertainties. As depicted in Fig. 2(a), the original CFBS controller and the disturbance observer based CFBS controller are tuned to achieve

Table 1 Vehicle parameters

Parameter	Value	Parameter	Value	Parameter	Value
A_b	2.223	A_{lat}	12.50	A_{lon}	141.08
B_a	2.448	B_{lat}	180.98	B_{lon}	-10.29
I_{xx}	0.305	I_{yy}	0.684	I_{zz}	0.787
L_a	55.86	L_b	708.02	M_a	345.19
M_b	-23.03	N_r	-11.445	N_{ped}	2095.16
N_{col}	256.42	τ	0.1078		

Table 2 Controller and observer gains

Controller gains	DO+CFBS	CFBS	Observer gains	
c_P	I_2	I_2	k_1, k_2	20
c_V	$2I_2$	$2I_2$	k_3, k_4	40
c_R	$10I_2$	$10I_2$	k_5, k_6	20
c_ω	$10I_2$	$100I_2$		
c_β	$10I_2$			

almost the identical trajectory. However, because the original CFBS controller ignores the transient response of flapping dynamics in quasi-steady approximation (5), a large gain in the last step ($c_w = 100I_2$) has to be adopted to deliver sufficient flapping angle moments and to achieve the fast regulation. Another difference between the two methods can be seen in cyclic inputs u_{lat} and u_{lon} from Fig. 2(b) where the original CFBS controller shows chattering control signals while those of the disturbance observer based CFBS controller are much smoother. Therefore, incorporating the

Table 3 Command filter parameters

No. of CF	Command variable	ω_n, deg/s	Mag. limit	Rate limit
CF_1	$V_{2,d}$	$287I_2$	$\pm 15I_2\, m/s$	$\pm 5I_2\, m/s^2$
CF_2	$R_{2,d}$	$1146I_2$	$\pm 0.8I_2$	$\pm 4I_2\, 1/s$
CF_3	$\omega_{2,d}$	$2005I_2$	$\pm 114.6I_2\, deg/s$	$\pm 573I_2\, deg/s^2$
CF_4	β_d	$3438I_2$	$\pm 8.595I_2\, deg$	$\pm 85.95I_2\, deg/s$

flapping angle estimates can help improve the control efficiency, reducing the workload of the servo actuators and increasing their life.

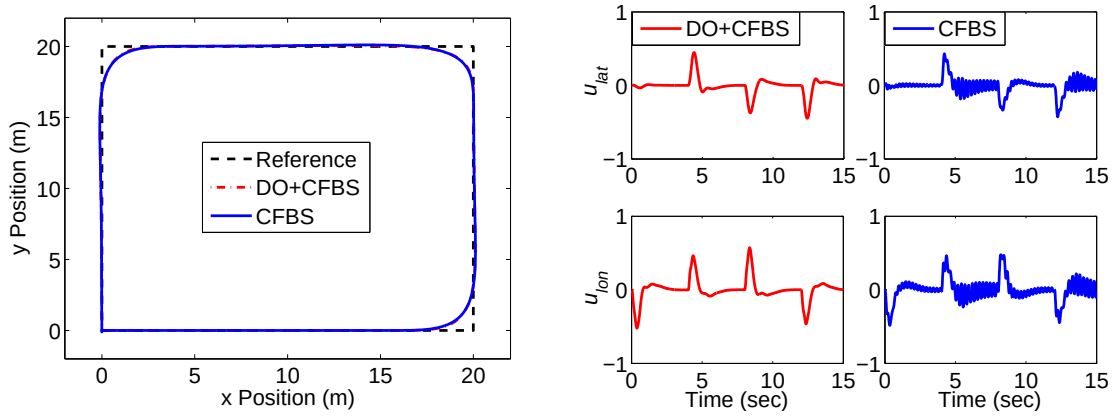

(a) (b)

Fig. 2 Comparison without disturbance and uncertainty

The second simulation demonstrates the anti-disturbance property of the proposed composite controller. It assumes 30% uncertainties on the aerodynamic coefficients, a constant wind disturbance of $5\,m/s$ acting on the helicopter, and a normalized lumped moment disturbance $d_{\bar{M}} = [172\,deg/s^2,\, 172\,deg/s^2]^T$. Degradation of the tracking performance of the original CFBS controller is visible in Fig. 3(a) while the tracking performance of the disturbance observer based CFBS controller is hardly affected by the disturbances and uncertainties. The difference between these two controllers is better revealed in the time history of the attitude angles in Fig. 3(b). Compared to the top plot, the bottom plot shows oscillations, which implies that the helicopter achieves better attitude stability with the disturbance observer based CFBS controller than with the original CFBS controller. Moreover, Fig. 3(d) shows that the disturbances and uncertainties aggravate the chattering of the control signals. Especially in the fourth segment when the helicopter is flying against the wind along its right side, the oscillations of the attitude angles and control signals are much severer. In contrast, the disturbance observer based CFBS controller retains the smooth control signals as shown in Fig. 3(c). Therefore, it can be concluded that the proposed disturbance observer based CFBS controller not only improves the control efficiency but also provides enhanced robustness against wind disturbances and parameter uncertainties.

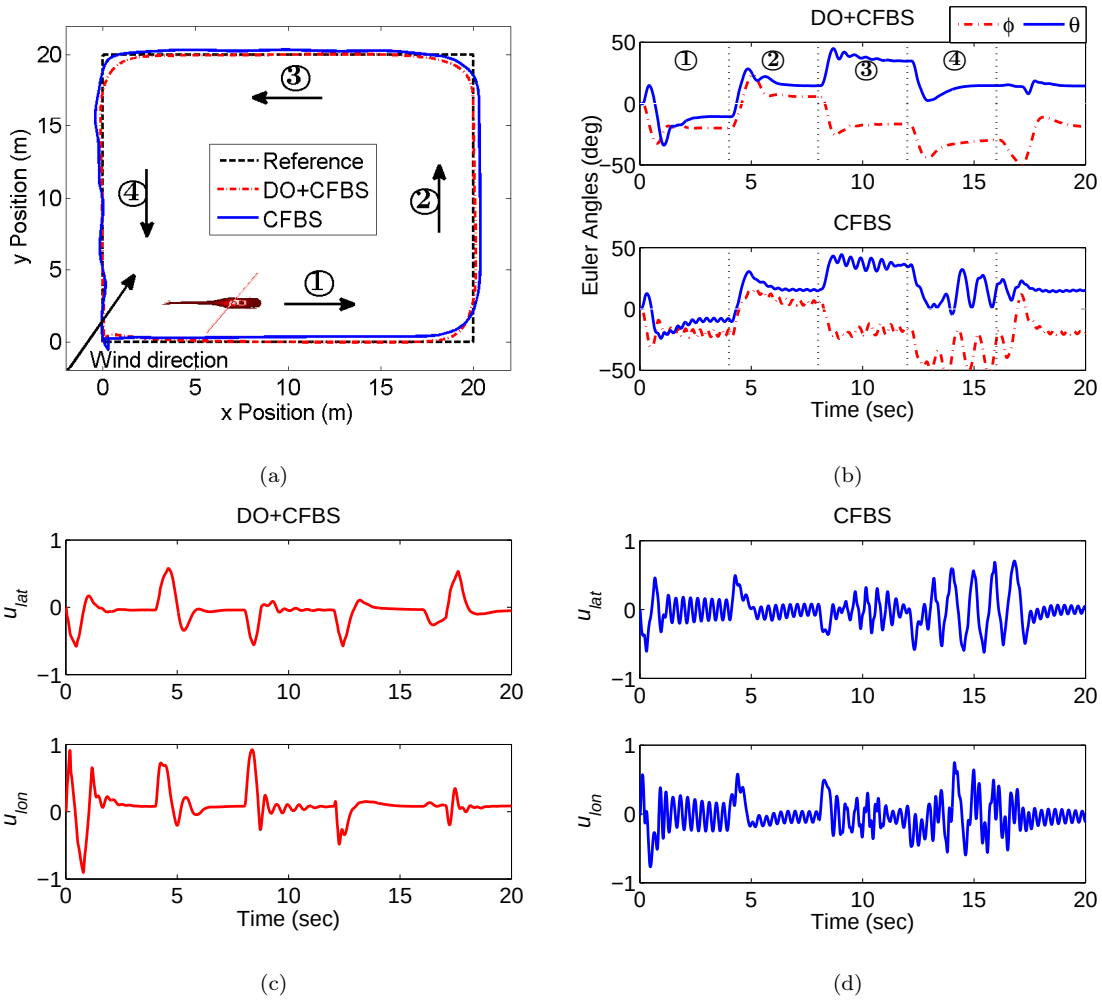

(a) (b) (c) (d)

Fig. 3 Comparison with disturbances and uncertainties

VII. Conclusion

This paper introduced a composite control strategy, namely disturbance observer based command filtered backstepping, for improved tracking control, as demonstrated for a small-scale helicopter. A novel disturbance observer is proposed to estimate the unmeasurable flapping angles and the lumped force and moment disturbances simultaneously. The acquired estimates are incorporated in a command filtered backstepping baseline controller to improve the control performance. The global asymptotic stability of the closed-loop system is established through the cascaded system analysis using the input-to-state stability property. Simulation results show that the proposed composite control strategy achieves better tracking performance and robustness against parameter uncertainties and wind disturbances. However, the more significant benefits of using the proposed

composite controller are the improvement of control efficiency, the reduction of demand on actuators, and the enhancement of attitude stability.

Acknowledgments

The authors would like to thank the associate editor and the reviewers for their constructive comments that significantly improved this note. This work was supported by National Basic Research Program of China (2012CB720003), National Natural Science Foundation of China (61127007, 61121003, and 61320106010). Hao Lu would like to thank the Chinese Scholarship Council for supporting his study in the United Kingdom.

References

[1] Chen, W.-H., "Nonlinear Disturbance Observer-Enhanced Dynamic Inversion Control of Missiles," *Journal of Guidance, Control, and Dynamics*, Vol. 26, No. 1, 2003, pp. 161–166, doi:10.2514/2.5027.

[2] Guo, L. and Chen, W.-H., "Disturbance Attenuation and Rejection for Systems with Nonlinearity via DOBC Approach," *International Journal of Robust and Nonlinear Control*, Vol. 15, No. 3, 2005, pp. 109–125, doi:10.1002/rnc.978.

[3] Li, S., Yang, J., Chen, W.-H., and Chen, X., *Disturbance Observer Based Control: Methods and Applications*, CRC Press, Boca Raton, FL, 2014, Chap. 1.

[4] Liu, C., Chen, W.-H., and Andrews, J., "Tracking Control of Small-Scale Helicopters Using Explicit Nonlinear MPC Augmented with Disturbance Observers," *Control Engineering Practice*, Vol. 20, No. 3, 2012, pp. 258–268, doi:10.1016/j.conengprac.2011.10.015.

[5] Cai, G., "Development of Small-Scale Unmanned-Aerial-Vehicle Helicopter Systems," Ph.D. Dissertation, Department of Electrical and Computer Engineering, National University of Singapore, Singapore, 2009, Chap. 4.

[6] Barczyk, M. and Lynch, A. F., "Control-Oriented Modeling of a Helicopter UAV with a Bell-Hiller Stabilizer Mechanism," *Proceedings of American Control Conference*, IEEE Publications, Piscataway, NJ, 2013, pp. 313-320, doi:10.1109/ACC.2013.6579856.

[7] Marconi, L. and Naldi, R., "Robust Full Degree-of-Freedom Tracking Control of a Helicopter," *Automatica*, Vol. 43, No. 11, 2007, pp. 1909–1920,
doi:10.1016/j.automatica.2007.03.028.

[8] He, Y. Q. and Han, J. D., "Acceleration-Feedback-Enhanced Robust Control of an Unmanned Helicopter," *Journal of Guidance, Control, and Dynamics*, Vol. 33, No. 4, 2010, pp. 1236–1250,
doi:10.2514/1.45659.

[9] Ahmed, B., Pota, H. R., and Garratt, M., "Flight Control of a Rotary Wing UAV Using Backstepping," *International Journal of Robust and Nonlinear Control Control*, Vol. 20, No. 6, 2010, pp. 639–658,
doi:10.1002/rnc.

[10] Zhu, B. and Huo, W., "Robust Nonlinear Control for a Model-Scaled Helicopter with Parameter Uncertainties," *Nonlinear Dynamics*, Vol. 73, No. 1-2, 2013, pp. 1139–1154,
doi:10.1007/s11071-013-0858-z.

[11] Peng, K., Cai, G., Chen, B. M., Dong, M., Lum, K. Y., and Lee, T. H. "Design and implementation of an autonomous flight control law for a UAV helicopter," *Automatica*, Vol. 45, No. 10, 2009, pp. 2333–2338,
doi:10.1016/j.automatica.2009.06.016.

[12] Raptis, I. A., Valavanis, K. P., and Vachtsevanos, G. J., "Linear Tracking Control for Small-Scale Unmanned Helicopters," *IEEE Transactions on Control Systems Technology*, Vol. 20, No. 4, 2012, pp. 995–1010,
doi:10.1109/TCST.2011.2158213.

[13] Peng, K., Chen, B. M., and Lum, K. Y., "Autonomous Flight Control Design for a Small-Scale Unmanned Helicopter," *AIAA Guidance, Navigation, and Control Conference*, AIAA paper 2011-6484, Reston, VA, August, 2011,
doi:10.2514/6.2011-6484.

[14] Farrell, J., Polycarpou, M., and Sharma, M., "Command Filtered Backstepping," *IEEE Transactions on Automatic Control*, Vol. 54, No. 6, 2009, pp. 1391–1395,
doi:10.1109/TAC.2009.2015562.

[15] Blanchini, F., Casagrande, D., Miani, S., and Viaro, U., "Stable LPV Realization of Parametric Transfer Functions and Its Application to Gain-Scheduling Control Design," *IEEE Transactions on Automatic Control*, Vol. 55, No. 10, 2010, pp. 2271–2281,
doi:10.1109/TAC.2010.2044259.

[16] Khalil, H. K., *Nonlinear Systems*, 3rd ed., Prentice-Hall, Upper Saddle River, NJ, 2002, Chap. 4.